https://doi.org/10.48048/tis.2022.6180

Magnetohydrodynamics (MHD) Induced Slip Flow of a Non-Newtonian Fluid through Circular Microchannels

Satyabrata Podder[1,*], Paulam Deep Paul[2] and Arunabha Chanda[1]

[1]Department of Mechanical Engineering, Jadavpur University, West Bengal 700032, India
[2]Department of Aerospace Engineering, University of Glasgow, Scotland, United Kingdom

([*]Corresponding author's e-mail: satyabrata1984@gmail.com)

Received: 30 June 2021, Revised: 14 September 2021, Accepted: 30 September 2021

Abstract

The present numerical analysis reveals the nature of non-Newtonian fluid flow through circular microchannels under slip boundary conditions. The power law has been used for the simulation of the fluid flow, which considers a steady, laminar, incompressible non-Newtonian fluid acted upon by a constant, externally applied magnetic field. The flow is axisymmetric and slip boundary conditions are applied in the near wall. A constant magnetic flux has been applied on the wall boundary to analyze the effect of magnetic field on Xanthan solution in formic acid, a type of non-Newtonian fluid having electrical conductivity. Using control volume method of finite difference scheme, a set of dimensionless governing differential equations defining the behavior of the fluid flow in the microchannel under an externally applied magnetic field, has been solved using slip boundary conditions to understand the effect of magnetic field on slip induced flow of non-Newtonian fluids. The results have depicted that the magnetic field affects both the centerline velocity and slip velocity but it is more prominent for the centerline velocities. The main objective of this research is to study the flow of non-Newtonian fluid, Xanthan through a circular microchannel and its corresponding behavior when flow boundary conditions are applied to interpret the characteristics under an externally applied magnetic field. The results obtained from this present study will find its application in the area of the flow of ferrofluids and biofluids.

Keywords: Magnetohydrodynamics, Non-Newtonian fluid flow, Microchannel, Navier-Stokes' equation, Slip flow

Nomenclature

B_0	Externally applied magnetic field (T)	z	Axial coordinate (m)
D	Diameter		**Greek symbols**
f	Friction factor, dimensionless	β	Slip coefficient, dimensionless ($= \frac{v_s}{v_m}$)
H_a	Hartmann No., dimensionless	γ	Shear rate (s^{-1})
k	Consistency index, kg $S^{(n-2)}$/m	η	Apparent viscosity (P_a. s)
l	Length of the microchannel	μ	Viscosity (P_a. s)
L	Length of the microchannel, dimensionless	ρ	Density (kg/m^3)
n	Flow behavior index, dimensionless	σ	Electrical conductivity ($(\Omega m)^{-1}$)
P	Pressure (Pa)	**τ**	Shear stress (N/m^2)
r	Radial coordinate, (m)		**Subscripts**
R_0	Radius of circular microchannel (m)	e	At entrance region
R_e	Reynolds number, dimensionless	h	Hydraulic quantity
R	Radius of the microchannel, dimensionless	max	Maximum value
u	Axial velocity (m/s)	m	Average value
v	Velocity (m/s)	r	Along r direction
V	Velocity, dimensionless	s	Slip value

Introduction

In last few decades, several experiments of micromachining and manufacturing of micro sized devices developed the application of micro-electro-mechanical-system (MEMS) in the various fields of engineering. Biomedical devices and mechanical systems of micro sizes have become more predominant in scientific experiments, industrial and commercial uses [1]. There is a significant development in the area of the fluid of various biological substances in biomedical devices which serves the requirement to analyze proteins [2], cells, DNA, embryos, blood [3], different chemical reagents and other similar substances. When these bio-fluids are allowed to pass through the channels of micro systems, they mostly show non-Newtonian single phase fluid flow in nature. The most common example of this type of flow through the micro-channels of micro-devices is blood. Microchannels offer advantages due to their high surface-to-volume ratio and their small volumes which lead to high rate of heat and mass transfer. Biological fluids have excellent match in length scale for substances like blood which is required to be allowed to pass through the micro channels of micro devices like lab on a chip device or micro filter for blood particle separation. Blood shows the value of consistency index (k) in the range of 16.08 to 16.26 and flow behavior index (n) in the range of 0.66 to 0.73 [4]. Numerical simulation of liquid flow in microchannels with experimental validation to predict and model pressure drops and losses in microchannels [5] shows that conventional theory can predict flow behavior in microchannels. Motion of the fluid at the vicinity of the microchannel wall is a popular area of research which shows that, there exists a non-linear relationship between the amounts of slip to the local shear rate at the solid-liquid interface through the use of simulations in molecular dynamics [6]. This change in local shear rate at wall leads to slip flow which depends upon the surface energy of the solid-liquid interface and other operational parameters like pressure drop [7], Reynolds No. [8] etc. and also in the thermal properties [9]. Both analytical [10] and numerical [11] approach is popular to find out the characteristics and nature of the slip flow of non-Newtonian fluids through microchannels. Surface energy of the solid-liquid interface plays a vital role in the slip flow. There have been various researches to explain slip in different molecular aspects like kinematic slip condition and van der Walls force [12], and thermal aspect like conjugate heat transfer and entropy generation [13]. The application of electric potential [14] in the flow of non-Newtonian fluids through microchannels, reveals that electro-viscosity plays different role for different flow behavior index. Slip flow as a physical phenomenon has attracted many researchers who study the subject to discuss about the application [15], nature [16] and the effects [17] of slip and slip boundary conditions. Depending upon the nature of the wall apparent slip appears for hydrophobic surface. Original slip boundary conditions, as provided by Navier have been tested numerically and experimentally. Boundary slip has always stabilised the flow while the consideration of apparent viscosity has destabilising effect by sharply reducing the boundary slip. The effect of slip has been studied for the different conditions for physical properties like viscoelasticity [18], shapes [19] or in the case of bi-phase flow [20]. In all the cases researchers find slip plays a vital role to explain the characteristics of the flow through microchannels. In the steady, pressure driven, 2-dimensional, Newtonian fluid flow at low Reynolds number limit the flow regime using Navier's slip boundary conditions [21]. The use of finite element simulations to study the effect of wall slip for the development of planar and axisymmetric Newtonian Poiseuille flow with Navier slip law varying linearly for slip velocity against wall shear stress showed the development length to be in good agreement with previous research done in the field [22]. Further study in this field develops a new approach towards coupling the equations between fluid-solid domains and has been validated by the data from previous studies with the impacts of parameters such as Knudsen No. [23] [24]. The analytical studies and modeling of slip flow of liquid in microchannels classified into velocity and other flow parameters [25]. The power law model is popular in the study of flow and thermal fields of non-Newtonian fluids in circular microchannels for numerical simulations The Poiseuille No. (f.Re) plays an important role for slip flow [26]. In the recent past, variation of flow boundary conditions from micro to nano scales becomes problematic to transport fluids using pressure gradients due to decrease in characteristic sizes. This led to the question of interface driven methods so as to look at flows near interfaces in order to reduce the flow friction [27]. Study of power-law rheology to describe the non-Newtonian characteristics of slip-flow of a nanofluid in a microtube is now a popular area of research. The consistency index and the flow behaviour index depend on the nanoparticle volume fraction has shown that the influence of nanoparticle volume fraction on the flow of the nanofluid depends on the pressure gradient, which is different from that of the Newtonian nanofluid [28]. Slip flow can be described by the term slip coefficient. For a non-Newtonian fluid, slip coefficient affects the flow [29]. The application of a constant, externally applied magnetic field on a microchannel is a popular area of research. The researches have showed the effect of externally applied magnetic field on the flow of

fluids [30,31] which are conductors of magnetism. Further studies have been conducted into the application of a constant magnetic field normal to the wall to find out the transport phenomena of Newtonian [32] or non-Newtonian [33] fluids. With the advent of the newly explored fluid characteristics of different materials with response to magnetism [34] attracts a scope of new research towards the MHD induced fluid flow of bio-fluids which are non-Newtonian in nature. There is a recent trend in this research area to add nanoparticles into the fluid under consideration. The introduction of nanoparticles shows enhancement in various fluid flow and heat transfer characteristics like convective heat transfer, exergy loss [35], Nusselt number [36] etc. Besides numerical analysis, homotopy perturbation method [37] and homotopy analysis method [38] is becoming popular in non-Newtonian fluid research which may be applied with proper boundary conditions. The present work shows the result of a non-Newtonian fluid flow, having an electrical conductivity through a circular straight microchannel. The flow considered in this analysis exhibits slip flow in near wall zone. An externally applied magnetic field has been applied normal to the microchannel wall in order to inspect the effects of MHD on the slip of the non-Newtonian fluid, Xanthan solution in formic acid.

Materials and methods

Physical considerations

A slip driven; non-Newtonian fluid flow has been considered through a circular microchannel. The diameter of the microchannel as compared to the length is very small. The fluid flowing through the microchannel is fully developed due to the sufficient length of the microchannel. The flow through the microchannel has been considered to be axisymmetric, laminar, steady, and incompressible in which Ostwald-deWaele power law model is used to analyze the behavior of non-Newtonian fluid. All the fluid properties are kept constant at the time of analysis. Slip boundary conditions is applied at the microchannel wall. The axial coordinate, z, is considered along the length of the channel and along the radial direction 'r' coordinate has been considered as shown in **Figure 1**. The flow is subjected to an external, constant magnetic field equal to a value varying from $B_0 = 0.1$T to 0.4T in order to determine the effect of increasing value of field intensity. This magnetic field is applied normal to the length of the microchannel. A unidirectional flow at the entry of the microchannel of intensity u_e is considered which is under the influence and application of an applied pressure gradient.

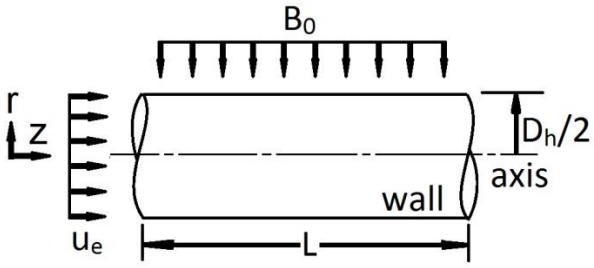

Figure 1 Schematic diagram of the flow field.

Power law model for a non-Newtonian fluid

The expression of Ostwald-deWaele model which is also known as power law is a mathematical description in generalized form for rheological fluids. This model has been used widely in the literatures [10,13] to model non-Newtonian fluids which relates the stress tensor (τ_{r_z}) with the shear rate ($\dot{\gamma}$) with the help of consistency factor (k) and flow behavior index (n). The expression of the power law for the unidirectional flow along the z axis can be written as:

$$\tau_{r_z} = k\left(\frac{dv_z}{dr}\right)^{n-1}\frac{dv_z}{dr} = \eta(\dot{\gamma}) \quad (1)$$

The apparent viscosity can be written as:

$$\eta = k\left(\frac{dv_z}{dr}\right)^{n-1} = k\dot{\gamma}^{(n-1)} \quad (2)$$

By assuming negligible influence of body force and other terms, the hydro-dynamically developed non-Newtonian flow with power-law model having constant properties throughout the computational domain in a circular microchannel (**Figure 1**) can be simplified to a simple form. The steady-state fully-developed flow of a power law fluid has been considered in the circular microchannel. The Navier Stokes equation in cylindrical co-ordinates along r-z direction for the given conditions can be expressed as:

$$\frac{\partial}{\partial r}(r\,\tau_{rz}) = -r\,\frac{\partial P}{\partial z} \tag{3}$$

Slip flow of non-Newtonian fluid

A solution of momentum equation has been done with slip boundary condition. From Eqs. (1) and (3) the solution of the given problem can be written as:

$$v_z = v_s + \left(\frac{3n+1}{n+1}\right)\left\{1 - \left(\frac{r}{R_0}\right)^{\frac{n+1}{n}}\right\}(v_m - v_s) \tag{4}$$

The following parameters in their non-dimensional form have been used to find out the non-dimensional form of velocity V.

$$\frac{V_z}{V_m} = V, \frac{r}{R_0} = R, \frac{l}{R_0} = L, \frac{v_s}{v_m} = \beta, \frac{z}{R_0} = Z, \frac{p}{\rho v_m^2} = P,\ Re = \frac{\rho\, v_m^{2-n} r_0^n}{k}$$

Using the above dimensionless quantities, Eq. (4) can be expressed as:

$$V = \beta + \left(\frac{3n+1}{n+1}\right)(1-\beta)\left(1 - R^{(n+1)/n}\right) \tag{5}$$

$$V_{max} = \beta + \left(\frac{3n+1}{n+1}\right)(1-\beta) \tag{6}$$

$$f.Re = 2^{(n+1)}\left(\frac{3n+1}{n}\right)^n (1-\beta)^n \tag{7}$$

Governing equations for fluid flow

The transport equations for the 2 dimensional, laminar and steady flows of the non-Newtonian fluids through a circular microchannel are written by considering a uniformly applied external magnetic field. Using r - z coordinate system the governing equations can be written in the dimensional form as: - Continuity equation:

$$\frac{\partial v_r}{\partial r} + \frac{\partial v_z}{\partial z} = 0 \tag{8}$$

Momentum equation:

$$\frac{\partial^2 v_z}{\partial r^2} + \frac{1}{r}\frac{\partial v_z}{\partial r} = \frac{-1}{\mu}\frac{\partial p}{\partial z} + \frac{\sigma}{\mu}B_0^2 v_z \tag{9}$$

Wall slip equation: For the momentum equation, Navier's slip condition is applied at the wall of the microchannel. This can be written as follows:

$$u_{s_{r = D_h/2}} = l_s\left(\frac{dv_z}{dr}\right)_{r = D_h/2} \tag{10}$$

Non-dimensional form of the governing equations

To make the governing equations dimensionless, the following quantities have been introduced.

$$R = \frac{r}{D_h};\ Z = \frac{z}{D_h};\ V_z = \frac{v_z}{v_{z_e}};\ G = \frac{\frac{dp}{dz}}{\frac{\rho v_{z_e}^2}{D_h}};\ H_a = B_0 D_h\sqrt{\frac{\sigma}{\mu}}$$

Therefore, the governing equations in the dimensionless form are given by:
Continuity equation:

$$\frac{\partial V_R}{\partial R} + \frac{\partial V_Z}{\partial Z} = 0 \tag{11}$$

Momentum equation:

$$\frac{\partial^2 V_Z}{\partial R^2} + \frac{1}{R}\frac{\partial V_Z}{\partial R} = R_e G + H_a^2 V_Z \tag{12}$$

Wall slip equation:

$$U_{s|_{R=1/2}} = L_s \left({}^{dV_z}/_{dR} \right) \tag{13}$$

Boundary condition

The Navier's slip boundary conditions are applied on the above equations to solve the physical problem. Slip boundary conditions can be summarised as follows:

$$\text{At } r = \frac{D_h}{2};\ v_z = v_s.\ \text{At } r = 0;\ \frac{dv_s}{dr} = 0. \tag{14}$$

The nondimensional form of the above slip boundary conditions can be written as follows:

$$\text{At } R = 1;\ V = \beta.\ \text{At } R = 0;\ \frac{dV}{dR} = 0. \tag{15}$$

Fluid properties

This work has been done by considering a fluid which exhibits simultaneous behaviour of non-Newtonian fluid and electrical conductivity. The present study reveals the fluid behaviour of Xanthan in formic acid solution (05 wt./vol%) when it is passed through a circular microchannel of sufficient length compared to the diameter. The properties of 0.5 wt./vol% xanthene polysaccharide are described in **Table 1**. The aqueous solution of Xanthan typically shows weal gel-like thixotropic properties. When this Xanthan mixed with formic acid in different ratio the solution shows electrical conductivity. Xanthan gum is a type of extracellular heteropolysaccharide produced by a bacterium called *Xanthomonas campestris*. It contains glucose, mannose and glucuronic acid in the molar ratio of 2:2:1.

Table 1 Properties of Xanthan solution in formic acid (25 °C) [34].

Xanthan [wt/vol%]	ρ (kg/m^3)	n	K ($kg\ s^{(n-2)}/m$)	Electrical conductivity (σ) $(\Omega m)^{-1}$
0.5	1225	0.761	0.214	0.01343

Numerical simulation

The fluid flow domain has been discretised and the equations of continuity and momentum are converted into the algebraic equations using 2000×10 grids. The present study involves 20000 elements and 22011 nodes to conduct the numerical tests. The flow field under consideration is 20 mm long circular microchannel having 200 μm radius. The actual number of meshes is finally selected on the basis of grid independence test for the final set of solution procedure. The total flow domain is discretized into non-overlapping rectangular mesh elements. For the solution of the governing equations, Semi-Implicit Method for Pressure Linked Equations, a numerical procedure used to solve the Navier-Stokes Equations. This algorithm is iterative in nature, where the boundary conditions are set up and the gradients of velocity and pressure are evaluated. The discretized momentum equation is used to compute the intermediate velocity field while mass fluxes at the faces are corrected and the pressure correction equation is solved to produce cell values of the pressure correction. The pressure field and boundary pressure corrections are then updated for each iterations thereby replacing the old values.

Validity and accuracy

The validity of the current work has been compared with the research work of Barkhordari and Etemad [26], where the simulation has been done in no-slip flow and slip flow regimes for values of slip coefficients ranging from 0 to 0.2. The results of the present work have been validated with the results of Sarabandi and Moghadam [23] for the velocity distribution of the fully developed power law fluid flow along the z-direction of the circular microchannel. The work justifies the result based on these values to validate the study and further improves upon it with the application of an externally applied magnetic field to present a novel approach towards the application in circular microchannel flow. **Figure 2** and **Table 2** represent the data accuracy and validation process for the present work. While there have been previous studies on microchannel [6], non-Newtonian flow [26,20] but the combination of slip flow [28] coupled with an externally applied magnetic field on a straight circular microchannel has not been taken up for study for applications pertaining to slip flow boundary conditions under MHD (Magneto hydrodynamics).

Stability and convergence

Numerical stability of the solution has been checked by the consistency of the finite difference equations derived from the governing equations of the present problem with help of the Eqs. (8) to (13). Errors generated from the finite difference approximation are in decreasing order as the computation proceeds from one iteration to the next. The convergence criteria for the present work have been set in the order of magnitude of 1×10^{-6}. On exceeding the value of 10^{-6}, the iteration terminates to achieve the solution of the numerical procedure. The value of convergence criteria is same for the equation of continuity for both r and z coordinates. The present problem uses absolute convergence criteria for the solution as the flow has been considered to be steady and laminar.

Results and discussion

The flow pattern of Xanthan solution in formic acid under different intensities of externally applied magnetic field was studied for different slip coefficients (β). The flow domain has been discretised which involves 20000 elements and 22011 nodes. The governing equations of continuity and momentum were converted into algebraic equations with the help of 10×2000 grids. The actual numbers of meshes were selected on the basis of mesh independence of the final solution. Before the final selection of mesh number across the flow field, a set of mesh sensitivity tests were done.

In order to check for accuracy, the results in **Figure 2** shows an excellent agreement with the available result for which n = 1.5, Re = 100, β = 0.2 with no externally applied magnetic field. Besides this a comparison of maximum velocity attained along the centreline (V_{max}) has been studied for slip and no slip conditions which is described in **Table 2**. When the flow deviates from no slip-to-slip flow regime, the axial velocity of the fluid has been found to increase at the vicinity of the wall. This phenomenon forces the fluid to decrease the corresponding centreline velocity in order to maintain the law of mass conservation.

Table 2 Centreline velocities (V_{max}) obtained for slip and no-slip conditions [Eq. (6)].

n	No Slip Flow		Slip Flow			
	β = 0.0		β = 0.1		β = 0.2	
	[Eq. (6)] [26]	Present Study	[Eq. (6)] [26]	Present Study	[Eq. (6)] [26]	Present Study
0.5	1.67	1.66	1.59	1.57	1.53	1.5
1.0	2.00	1.99	1.89	1.9	1.79	1.8
1.25	2.11	2.07	2.00	1.96	1.88	1.86

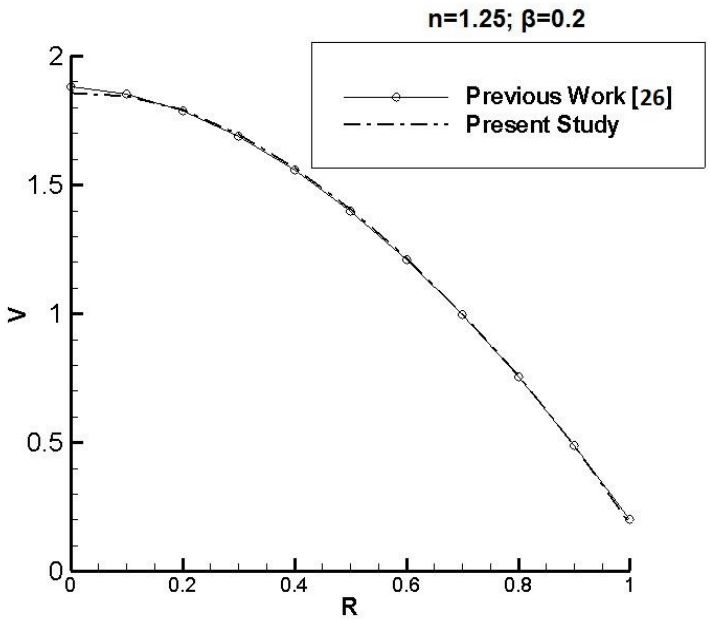

Figure 2 Comparison of velocity profiles obtained in present work and previous studies.

Slip is a near wall phenomenon which can be quantified by the changing nature of the Re value as the microchannel flow shifts from no-slip to slip flow regime. The deviation of flow from no slip to slip observes the wall shear stress to decrease with the increment of wall velocity. The quantification of this change majorly depends on the slip coefficient. When the flow entered into the fully developed region of the microchannel, it has been observed that the shear stress at the wall decreases with the increase in slip coefficient. When the value of slip coefficient is in the higher order, the wall velocity increases and tends to approach the value of centreline velocity. The range of slip coefficient has been selected in order to determine the slip flow regime at the near wall zone for the values when the fluid flow begins to deviate from no slip to slip flow. The velocity at the wall and centreline, along with their corresponding wall shear stress has been found to be linear for the higher values of slip coefficient. The present work is focused on the range of slip coefficient up to the value of 0.3 The Slip phenomena is more prominent when wall shear stress decreases and β increases (**Table 3**).

Table 3 f.Re values obtained from present work and previous studies for slip and no-slip conditions [Eq. (7)].

n	No Slip Flow		Slip Flow			
	β = 0.0		β = 0.1		β = 0.2	
	[Eq. (7)] [26]	Present Study	[Eq. (7)] [26]	Present Study	[Eq. (7)] [26]	Present Study
0.5	6.32	6.31	5.97	5.80	5.63	5.72
1.0	16.00	15.95	14.31	14.12	12.72	12.20
1.25	25.24	25.10	21.95	22.25	18.95	20.26

A comparison of different dimensionless velocity profiles has been shown in **Figure 3** for no slip (β = 0.0) and various slip flow coefficients when no magnetic field is applied and flow behaviour index value at n = 0.761. It is observed that with the increasing value of β, the velocity of the fluid at the vicinity of the wall increases and the centreline velocity decreases. In contrast, with slip condition, the velocity gradient decreases at near wall region for higher values of slip coefficient β, in order to preserve the law of mass conservation. A plug like velocity profile is observed.

For the given fluid, when magnetic fields of various intensities are applied on the slip flow boundary conditions, it is observed that with the increasing value of magnetic field intensity, the

centreline velocity increases. In **Figure 4** a comparison is made between various dimensionless velocity profiles when the slip coefficient β is maintained at a constant value of 0.2. The slip velocity also differs at the microchannel wall with the change of increasing intensities of externally applied magnetic field but that change is very insignificant.

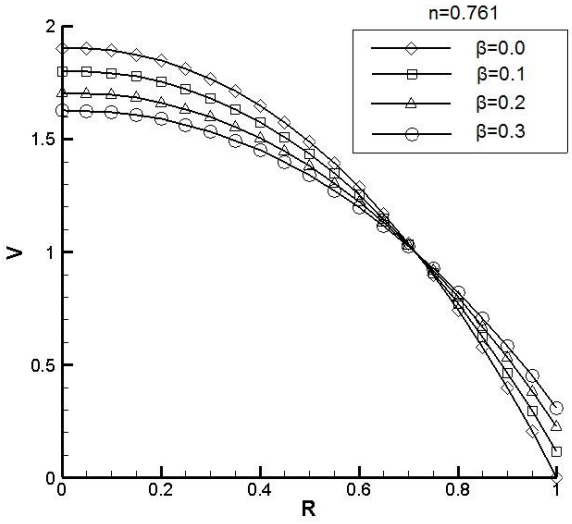

Figure 3 Comparison of velocity profiles of slip and no slip flows for different values of slip co-efficient (β) when no magnetic field is applied.

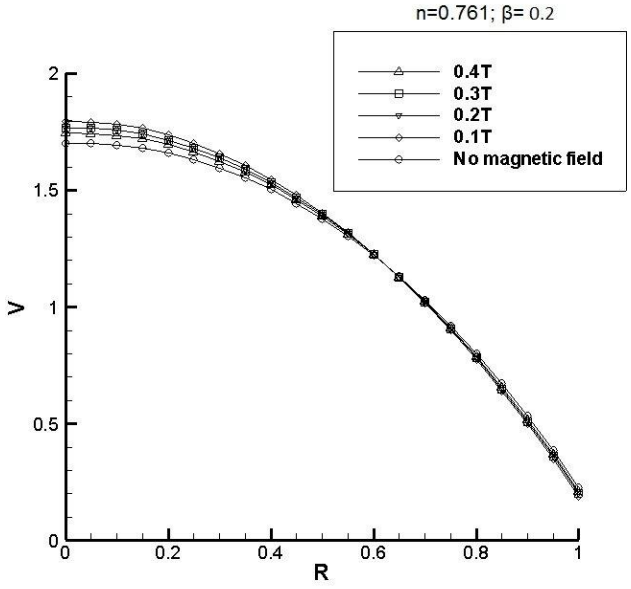

Figure 4 Comparison of velocity profiles for different values of applied magnetic field (B_0) when slip co-efficient (β) is 0.2.

A comparison of different flow patterns due to different values of slip coefficients have been done by plotting the corresponding velocity profiles (**Figure 5**) when exposed to an externally applied magnetic field of same intensity (0.3T). The plot shows a tendency, that with the increase in slip

coefficient, slip velocity increases and the corresponding centerline velocity decreases, in order to conserve the momentum of the flow in the microchannel.

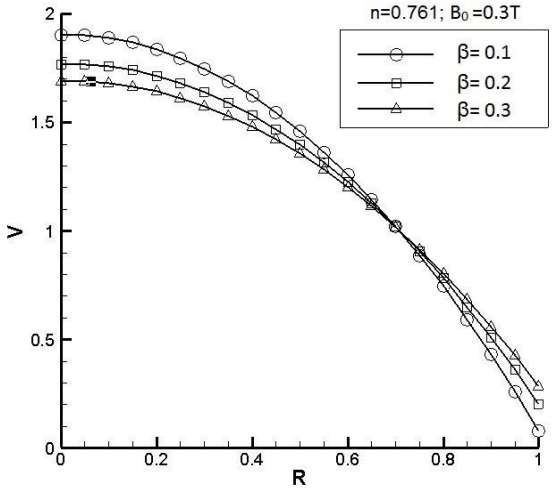

Figure 5 Comparison of velocity profiles for the different values of β when applied magnetic field (B_0) is held constant to 0.3T.

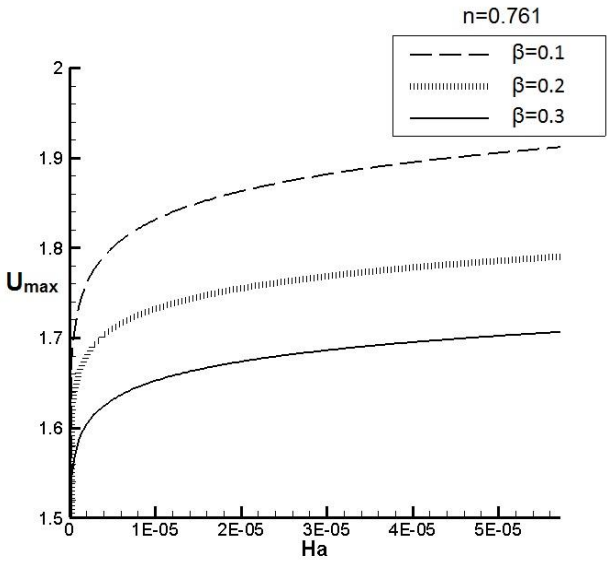

Figure 6 Effect of Hartmann no. (Ha) on U_{max}.

The effect of an externally applied magnetic field on the centerline velocity in the microchannel is shown in **Figure 6**. The electromagnetic force becomes predominant in comparison to viscous force with the increment in Hartmann no. (Ha), this increases the centerline velocity of the fluid flow having different slip coefficients. The effect of externally applied magnetic field on the slip velocity, near the wall shows the opposite tendency. With the increment in Hartmann no. (Ha), slip velocity decreases rapidly to a certain value of 1.5×10^{-5} and at the later stage this influence becomes less significant and the curve becomes asymptotic. This behavior is shown in **Figure 7** below, where the effect of magnetic field dominates the centerline velocity more in comparison to slip velocity in the microchannel.

The Hartman number depicts the relation between electromagnetic force and viscous force when the field intensity and characteristic length is considered constant. For a given slip coefficient, the slip velocity decreases with increase in Hartman number which demonstrates the dominance of electromagnetic force over viscous force. The value of slip velocity is higher for slip coefficients having higher values for the corresponding Hartman number. This trend in slip velocity decreases over the decrement in the slip coefficient value as the flow tends towards the no slip boundary conditions at the microchannel wall which reinstates the general flow behavior in the absence of slip flow boundary conditions.

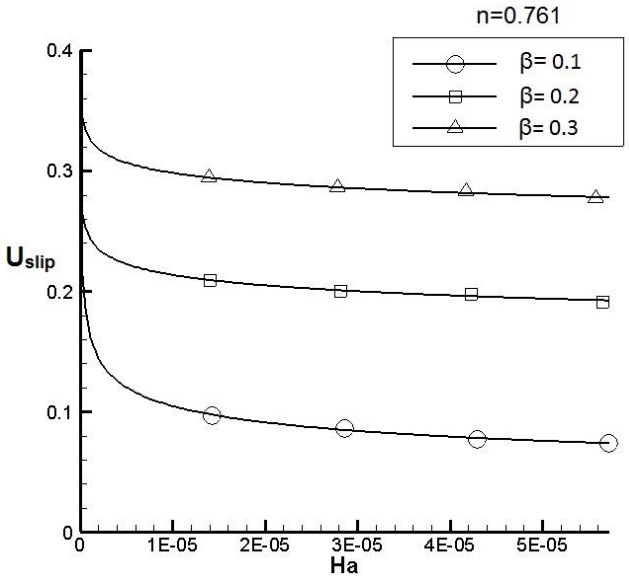

Figure 7 Effect of Hartmann no. (Ha) on $U_{slip.}$

When comparing the relation between β and Ha, the result reveals that by the increasing value of Ha, slip coefficient decreases. This tendency is much prominent in the region where β is less. With the increment of β this tendency decreases (**Figure 8**).

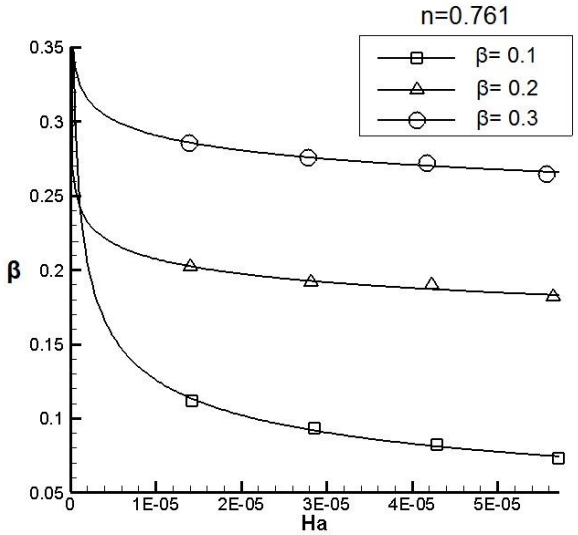

Figure 8 Effect of Hartmann no. (Ha) on Slip co-efficient (β).

Figure 9 depicts a graphical representation of centerline velocity for different β when they are exposed to a same $B_0 = 0.4T$. This diagram shows the gradual development of the flow along the microchannel and at the 20 % microchannel length flow develops to be a fully developed flow on which the electromagnetic force is applied. For the given conditions, the fluid flow having less β exhibits maximum centerline velocity.

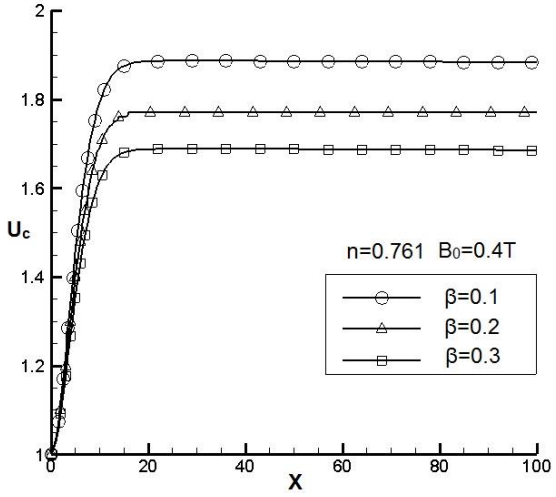

Figure 9 Comparison of U_c v/s X for $B_0 = 0.4T$ for the different values of β.

In **Figure 10** a comparison of f.Re values for the different β to find out the fact that, when β is less f.Re becomes more which makes the slip velocity less. But opposite happens with the increase in β and consequently f.Re decreases and slip velocity increases.

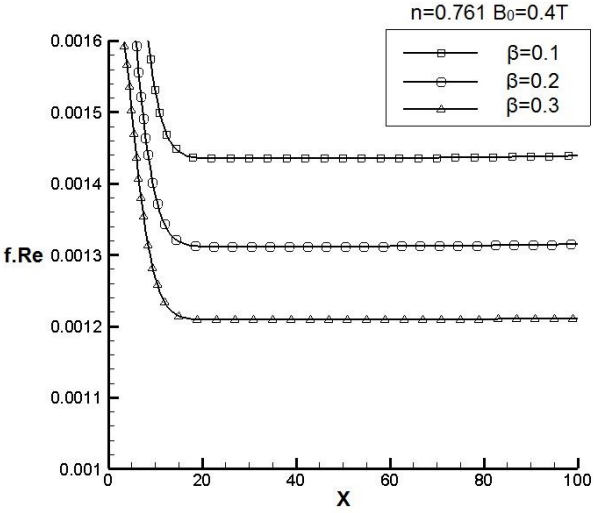

Figure 10 Comparison of f.Re v/s X for $B_0 = 0.4T$ for the different values of β.

A comparison in the values of V_{max} and V_{slip} is drawn in **Tables 4** and **5** for the different values of β and applied magnetic field. When externally applied magnetic field is acted on the flow then slip flow decreases and corresponding centerline velocity increases in each case to maintain the momentum balance. The comparison for maximum centerline velocity under different magnetic field intensity with varying slip coefficient reveals the relative change of the maximum centerline velocity when the field

intensity has been increased from 0T to 0.4T for different values of slip coefficients. The percentage increase of maximum centerline velocity for a specified slip coefficient on increasing the field intensity is shown on **Table 4** where a change of 6.1 % is observed for the slip coefficient of 0.1 when the field intensity was increased from 0T to 0.4T. Similar comparison has been represented in **Table 5** for slip velocity near microchannel walls where for a given value of slip coefficient of 0.1, the increasing field intensity records a decrease in the slip velocity with 32.73 % with the variation of field intensity from 0T to 0.4T.

Table 4 Comparison of the developed U_{max} for different MHD.

Varying Magnetic Field intensities (B_0)	**Varying Slip Coefficient (β)**		
	0.1	**0.2**	**0.3**
0	1.80	1.70	1.62
0.1T	1.84	1.75	1.66
0.2T	1.88	1.76	1.68
0.3T	1.90	1.77	1.69
0.4T	1.91	1.79	1.71
Relative difference % = $\frac{(U_{max})_{B_0 = 0.4T} - (U_{max})_{B_0 = 0.0T}}{(U_{max})_{B_0 = 0.0T}} \times 100$	6.1	5.9	5.6

Table 5 Comparison of the developed U_{slip} for different MHD.

Varying Magnetic Field intensities (B_0)	**Varying Slip Coefficient (β)**		
	0.1	**0.2**	**0.3**
0	0.110	0.225	0.308
0.1T	0.098	0.209	0.294
0.2T	0.086	0.200	0.286
0.3T	0.077	0.198	0.283
0.4T	0.074	0.191	0.277
Relative difference % = $\frac{(U_{slip})_{B_0 = 0.4T} - (U_{slip})_{B_0 = 0.0T}}{(U_{slip})_{B_0 = 0.0T}} \times 100$	32.73	15.11	10.06

Conclusions

The current work studies the effect of an externally applied magnetic field of varying intensities on slip flow of Xanthan solution through a circular straight microchannel. The results obtained from the simulation of a non-Newtonian fluid (Xanthan) concludes the increment of centerline velocity in slip boundary conditions under the action of an externally applied magnetic field while the corresponding slip velocity near the microchannel wall region decreases. The effect of the magnetic field is more dominating on the centerline flow velocities compared to the near wall region. The Lorentz force of electromagnetism acts as a resistive force for the fluid flow through the microchannel. This resistive force reduces the velocity at the vicinity of the microchannel walls, in accordance with the law of conservation of momentum of the fluid flow through the microchannel. The comparison for maximum centerline velocity under different magnetic field intensity with varying slip coefficient reveals the relative change of the maximum centerline velocity when the field intensity has been increased, for different values of slip coefficients. Similar comparison has been represented for slip velocity near microchannel walls where for a given value of slip coefficient, the increasing field intensity records a decrease in the slip velocity, with the variation of field intensity. It has been observed that the values for U_{max} and U_{slip} has increased and decreased respectively for different values of slip coefficients under varying magnetic field when compared to the results with no external field intensity. From the various comparisons it can be concluded that the effect of externally applied magnetic field is more prominent in near wall region than that of centerline of the microchannel. This tendency decreases for both centerline velocity and slip velocity when slip coefficient increases.

Acknowledgement

The Authors would like to thank and acknowledge the support of Jadavpur University, Kolkata, India for their kind approval to use the laboratory set ups and other academic resources of the university for the requirement of the present work. The authors are also grateful to the anonymous reviewers for their constructive comments for the development of the work.

References

[1] M Gad-el-Hak. The fluid mechanics of microdevices - the freeman scholar lecture. *J. Fluids Eng.* 1999; **121**, 5-33.
[2] L Bazinet, M Trigui and D Ippersiel. Rheological Behaviour of WPI dispersion as a function of pH and protein concentration. *J. Agric. Food Chem*. 2004; **52**, 5366-71.
[3] S Chakraborty. Dynamics of capillary flow of blood into a microfluidic channel. *Lap Chip* 2005; **5**, 421-30.
[4] MA Elblbesy and AT Hereba. Computation of the coefficients of the power law model for whole blood and their correlation with blood parameters. *Appl. Phys. Res.* 2016; **8**, 1.
[5] D Liu and SV Garimella. Investigation of liquid flow in microchannels. *CTRC Res. Publ*. 2004. http://docs.lib.purdue.edu/coolingpubs/295.
[6] PA Thompson and SM Troian. A general boundary condition for liquid flow at solid surfaces. *Nature* 1997; **389**, 360-2.
[7] X Yang, NT Weldetsadik, Z Hayat, T Fu, S Jiang, C Zhu and Y Ma. Pressure drop of single-phase flow in microchannels and its application in characterizing the apparent rheological property of fluids. *Microfluid. Nanofluid*. 2019; **23**, 75.
[8] X Zhang, F He, P Hao, Y Gao, L Sun, Xi Wang and X Jin. Experimental investigation of flow characteristics for liquid flow in microchannels at very low Reynolds numbers. *Chem. Eng. Technol*. 2016; **39**, 1425-30.
[9] AH Sarabandi and AJ Moghadam. Thermal analysis of power-law fluid flow in a circular microchannel. *J. Heat Transf*. 2017; **139**, 032401.
[10] YS Muzychka and J Edge. Laminar non-Newtonian fluid flow in noncircular ducts and microchannels. *J. Fluids Eng.* 2008; **130**, 111201.
[11] K Vajravelu, JR Cannon and D Rollins. Analytical and numerical solutions of nonlinear differential equations arising in non-Newtonian fluid flows. *J. Math. Anal. Appl*. 2000; **250**, 204-21.
[12] LM Pismen and BY Rubinstein. Kinetic slip condition, van der Waals forces, and dynamic contact angle. *Am. Chem. Soc.* 2001; **17**, 5265-70.
[13] R Sarma, H Gaikwad and PK Mondal. Effect of conjugate heat transfer on entropy generation in slip-driven microflow of power law fluids. *Nanoscale Microscale Thermophys. Eng.* 2017; **21**, 26-44.
[14] GH Tang, PX Ye and WQ Tao. Electro viscous effect on non-Newtonian fluid flow in microchannels. *J. Non-Newton Fluid Mech*. 2010; **165**, 435-40.
[15] H Brenner. Beyond the no-slip boundary condition. *Am. Phys. Soc. Phys. Rev*. 2011; **84**, 046309.
[16] DC Tretheway and CD Meinharta. Apparent fluid slip at hydrophobic microchannel walls. *Phys. Fluids* 2001; **14**, L9.
[17] XY You, JR Zheng and Q Jing. Effects of boundary slip and apparent viscosity on the stability of microchannel flow. *Forsch. Ingenieurwes*. 2007; **71**, 99-106.
[18] LL Ferras, AM Afonso, MA Alves, JM Nobrega, OS Carneiro and FT Pinho. Slip flows of Newtonian and viscoelastic fluids in a 4:1 contraction. *J. Non-Newton Fluid Mech*. 2014; **214**, 28-37.
[19] M Shojaeian and SAR Dibaji. Three-dimensional numerical simulation of the slip flow through triangular microchannels. *Int. Commun. Heat Mass Transf*. 2010; **37**, 324-9.
[20] MH Mansour, A Kawahara and M Sadatomi. Experimental investigation of gas-non-Newtonian liquid two-phase flows from T-junction mixer in rectangular microchannel. *Int. J. Multiph. Flow* 2015; **72**, 263-74.
[21] CS Nishad, A Chandra and GPR Sekhar. Flows in slip-patterned micro-channels using boundary element methods. *Eng. Anal. Bound. Elem*. 2016; **73**, 95-102.
[22] Z Kountouriotis, M Philippou and GC Georgiou. Development lengths in Newtonian Poiseuille flows with wall slip. *Appl. Math. Comput.* 2016; **291**, 98-114.
[23] AH Sarabandi and AJ Moghadam. Thermal analysis of power-law fluid flow in a circular microchannel. *J. Heat Transf*. 2017; **139**, 032401.

[24] MRS Bushehri, H Ramin and MR Salimpour. A new coupling method for slip-flow and conjugate heat transfer in a parallel plate micro heat sink. *Int. J. Therm. Sci*. 2015; **89**, 174-84.
[25] N Kashaninejad, WK Chan and NT Nguyen. Analytical modeling of slip flow in parallel-plate microchannels. *Micro Nanosyst.* 2013; **5**, 245-52.
[26] M Barkhordari and SG Etemad. Numerical study of slip flow heat transfer of non-Newtonian fluids in circular microchannels. *Int. J. Heat Fluid Flow* 2007; **28**, 1027-33.
[27] L Bocquet and JL Barrat. Flow boundary conditions from nano- to micro-scales. *Soft Matter* 2007; **3**, 685-93.
[28] J Niu, C Fu and W Tan. Slip-flow and heat transfer of a non-Newtonian nanofluid in a microtube. *PLoS One* 2012; **7**, e37274.
[29] SA Sajadifar, A Karimipour and D Toghraie. Fluid flow and heat transfer of non-Newtonian nanofluid in a microtube considering slip velocity and temperature jump boundary conditions. *Eur. J. Mech. B Fluids* 2017; **61**, 25-32.
[30] HF Oztop, K Al-Salem and I Pop. MHD mixed convection in a lid-driven cavity with corner heater. *Int. J. Heat Mass Transf.* 2011; **54**, 3494-504.
[31] KM Rabbi, S Saha, S Mojumder, MM Rahman, R Saidur and TA Ibrahim. Numerical investigation of pure mixed convection in a ferrofluid-filled lid-driven cavity for different heater configurations. *Alex. Eng. J.* 2016; **55**, 127-39.
[32] G Nagarajua, M Garvandha and JVR Murthy. MHD flow in a circular horizontal pipe under heat source/sink with suction/injection on wall. *Front. Heat Mass Transf.* 2019; **13**, 6.
[33] M Kiyasatfar and N Pourmahmoud. Laminar MHD flow and heat transfer of power-law fluids in square microchannels. *Int. J. Therm. Sci*. 2016; **99**, 26-35.
[34] E Shekarforoush, A Faralli, S Ndoni, AC Mendes and IS Chronakis. Electrospinning of Xanthan polysaccharide. *Macromol. Mater. Eng*. 2017; **302**, 1700067.
[35] M Sheikholeslami and SA Farshad. Investigation of solar collector system with turbulator considering hybrid nanoparticles. *Renew. Energy* 2021; **171**, 1128-58.
[36] TG Ashrafi, S Hoseinzadeh, A Sohani and MH Shahverdian. Applying homotopy perturbation method to provide an analytical solution for Newtonian fluid flow on a porous flat plate. *Math. Methods Appl. Sci*. 2021; **44**, 7017-30.
[37] S Hoseinzadeh, PS Heyns and H Kariman. Numerical investigation of heat transfer of laminar and turbulent pulsating Al_2O_3/water nanofluid flow. *Int. J. Numer. Methods Heat Fluid Flow* 2020; **30**, 1149-66.
[38] S Hoseinzadeh, PS Heyns, AJ Chamkha and A Shirkhani. Thermal analysis of porous fins enclosure with the comparison of analytical and numerical methods. *J. Therm. Anal. Calorim.* 2019; **138**, 727-35.